The FASEB Journal article fj.13-235440. Published online December 10, 2013.

Unexpected low-dose toxicity of the universal solvent DMSO

Joana Galvao,* Benjamin Davis,* Mark Tilley,* Eduardo Normando,*,§ Michael R. Duchen,†,‡ and M. Francesca Cordeiro*,§,1

*Glaucoma and Retinal Neurodegeneration Research Group, Institute of Ophthalmology, †Department of Cell and Developmental Biology, and ‡UK Parkinson's Disease Consortium, Institute of Neurology, University College London, London, UK; and §Western Eye Hospital, Imperial College, London, UK

ABSTRACT **Dimethyl sulfoxide (DMSO) is an important aprotic solvent that can solubilize a wide variety of otherwise poorly soluble polar and nonpolar molecules. This, coupled with its apparent low toxicity at concentrations <10%, has led to its ubiquitous use and widespread application. Here, we demonstrate that DMSO induces retinal apoptosis *in vivo* at low concentrations (5 μl intravitreally dosed DMSO in rat from a stock concentration of 1, 2, 4, and 8% v/v). Toxicity was confirmed *in vitro* in a retinal neuronal cell line, at DMSO concentrations >1% (v/v), using annexin V, terminal deoxynucleotidyl transferase dUTP nick end labeling (TUNEL), 3-(4,5-dimethylthiazol-2-yl)-2,5-diphenyltetrazolium bromide (MTT), and AlamarBlue cell viability assays. DMSO concentrations >10% (v/v) have recently been reported to cause cellular toxicity through plasma membrane pore formation. Here, we show the mechanism by which low concentrations (2–4% DMSO) induce caspase-3 independent neuronal death that involves apoptosis-inducing factor (AIF) translocation from mitochondria to the nucleus and poly-(ADP-ribose)-polymerase (PARP) activation. These results highlight safety concerns of using low concentrations of DMSO as a solvent for *in vivo* administration and in biological assays. We recommend that methods other than DMSO are employed for solubilizing drugs but, where no alternative exists, researchers compute absolute DMSO final concentrations and include an untreated control group in addition to DMSO vehicle control to check for solvent toxicity.—Galvao, J., Davis, B., Tilley, M., Normando, E., Duchen, M. R., Cordeiro, M. F. Unexpected low-dose toxicity of the universal solvent DMSO. *FASEB J.* 28, 000–000 (2014). www.fasebj.org**

Key Words: neuronal apoptosis · retina · DARC · toxicity · AIF

Dimethyl sulfoxide [$(CH_3)_2S$; DMSO] is an organic polar aprotic molecule widely used as a solvent for the dissolution of small hydrophobic drug molecules due to its amphipathic nature (1). DMSO is commonly utilized for cell cryopreservation because of its membrane penetrating and water displacement properties. Due to its broad solubilizing capability, DMSO is employed as a solvent for many drug types and is often used as the vehicle control-of-choice for both *in vitro* and *in vivo* studies (2–4). While some studies recognize that DMSO can be toxic (5, 6), so ubiquitous is the use of this solvent that the concentration of DMSO used is often unreported (2, 3). A similar disregard for its potency is observed *in vivo*, where systemic DMSO injections have been used as vehicle controls for: peripheral nerve regeneration (7), silencing gene expression (8, 9), inhibition of tumor growth (10), and compression-induced muscle damage (11). In the eye, DMSO has also been used as a topical vehicle control (12), including a clinical study in 1975 in which 50% (v/v) DMSO was applied topically twice daily for 2 yr (13). Furthermore, subconjunctival administration of 80% (v/v) DMSO was used as a control for both rapamycin treatment (14) and following trabeculectomy (15). Most often, however, DMSO is administered intravitreally (IVT) as a vehicle control in animal studies, including for: curcumin (5 pmol, 20 pmol; ref. 16), rotenone (0.2 mg/kg in DMSO, with DMSO vehicle controls; refs. 17, 18), 2-(6-cyano-1-hexyn-1-yl)

Abbreviations: AIF, apoptosis-inducing factor; ARPE 19, human retinal pigment epithelial cell line; cFLIP(L), cellular FLICE-inhibitory protein; CsA, cyclosporine A; Bax, Bcl-2-ssociated X protein; DARC, detection of apoptosing retinal cells; DMSO, dimethyl sulfoxide; FADD, Fas-associated protein with death domain; Fluo-4 AM, 2-{[2-(2-{5-[bis(carboxymethyl)amino]-2-methylphenoxy}ethoxy)-4-(2;7-difluoro-6-hydroxy-3-oxo-3H-xanthen-9-yl)phenyl](carboxymethyl)amino}acetic acid; IAP, inhibitor of apoptosis proteins; IVT, intravitreally; MNNG, methylnitronitrosoguanidine; mPTPm mitochondrial permeability transition pore; MTT, 3-(4,5-dimethylthiazol-2-yl)-2,5-diphenyltetrazolium bromide; PARP, poly(ADP-ribose)polymerase; PI, propidium iodide; RGC, retinal ganglion cell; TUNEL, terminal deoxynucleotidyl transferase dUTP nick end labeling; Z-DEVD-fmk, benzyloxycarbonyl-Asp(OMe)-Glu(OMe)-Val-Asp(OMe)-fluoromethylketone

[1] Correspondence: Glaucoma and Retinal Neurodegeneration Research Group, Institute of Ophthalmology, University College London, London EC1V 9EL, UK. E-mail: m.cordeiro@ucl.ac.uk

doi: 10.1096/fj.13-235440

adenosine [2-CN-Ado, 50% (v/v) DMSO; ref. 19], and histone H4 deacetylation DMSO (1 μl; ref. 8).

Apoptosis, or programmed cell death, plays an essential role in homeostasis and the normal development of all multicellular organisms; in fact dysregulation of this process is responsible for a plethora of autoimmune and neurodegenerative diseases (20). Mitochondria play a central role in the regulation of apoptosis and are involved in the release or interaction with different pro- and antiapoptotic proteins that trigger both caspase-dependent and caspase-independent cell death (21, 22).

In vitro, DMSO is reported to induce apoptosis at concentrations >10% (v/v), due to plasma membrane pore formation (23, 24). Moreover, DMSO has been previously reported to induce cell death through caspase-9 in the EL-4 cell line and caspase-3 activation both *in vitro* in a cochlear cell line and *in vivo* in the developing central nervous system (6, 25, 26).

This study aims to establish whether the use of DMSO as a vehicle control in ocular drug delivery is fit for purpose. This was investigated by evaluating its effects in the retina *in vivo* and *in vitro* at DMSO concentrations <10% (v/v).

MATERIALS AND METHODS

Animals

Adult, male, Dark Agouti rats (Harlan Laboratories, Bicester, UK) weighing 150–200 g were housed in an air-conditioned, 21°C environment with a 12 h light-dark cycle (50 lux), where food and water were available *ad libitum*. All the experimental and animal care procedures were approved by the UK Home Office and in compliance with the Association for Research in Vision and Ophthalmology Statement for the Use of Animals in Ophthalmic and Vision Research.

Intravitreal injections

All animals were anesthetized by intraperitoneal injection using a mixture of ketamine (37.5%)/medetomidine (25% Dormitor; Pfizer Animal Health, Exton, PA, USA) solution (0.75 ml ketamine, 0.5 ml medetomidine, and 0.75 ml sterile water) at 0.2 ml/100 g as described previously (27). Animals were randomly assigned to DMSO treatment (5 μl stock at 0, 1, 2, 4, 8, 10, 15, and 25%; minimum of $n=4$ eyes/concentration). A final volume of 5 μl DMSO and fluorescently labeled annexin V (Anx-F) was administered IVT (27) using a 34-gauge needle attached to a 5-μl Hamilton syringe (Hamilton, Reno, NV, USA) under direct microscopic visualization. The needle was inserted through the sclera superiorly, 1 mm behind the limbus, at an angle of 45° (27), and caution was taken to avoid contact with the lens.

In vivo imaging of externalization of phosphatidylserine of retinal ganglion cell (RGC) apoptosis

Eyes were imaged using an Heidelberg Retinal Angiograph (HRA) Spectralis (Heidelberg Engineering, Heidelberg, Germany) as described previously (27). Preliminary experiments established the effects of DMSO to be optimal 2 h after injection IVT. Pupils were dilated with 1 drop each of phenylephrine hydrochloride 2.5% and cyclopentolate hydrochloride 1.0%, and corneal clarity was preserved with regular lubrication. During image acquisition, the HRA Spectralis was focused on the retinal nerve fiber layer, as identified in the reflectance mode. The images were collected and analyzed using a recently validated MatLab script [validation and refinement of an automated technique of counting apoptosing retinal cells imaged with detection of apoptosing retinal cells (DARC); ref. 28].

Cell culture

A transformed RGC-5 cell line was used in this study, which was a kind gift from Dr. Neeraj Agarwal (Department of Cell Biology and Genetics, University of North Texas Health Science Center, Fort Worth, TX, USA). This cell line has been characterized as expressing the RGC proteins Thy-1 and Brn-3c (29), and we have confirmed that they express the RGC marker Brn3a as well as the neuronal marker β3 tubulin (16, 30). The original cell line was transformed with Ψ2 E1A virus and developed from postnatal Sprague-Dawley rats (29), but recent controversy has suggested they may be derived from mice (31). However, they remain the only cell line that resembles RGCs and are repeatedly used in this manner (32, 33). RGC-5 were grown in Dulbecco's modified Eagle's medium (DMEM; Invitrogen, Paisley, UK), supplemented with 10% heated-inactivated fetal bovine serum (Invitrogen), 100 U/ml penicillin, and 100 mg/ml streptomycin.

In vitro imaging of externalization of phosphatidylserine in RGC-5 apoptosis

RGC-5 cells were seeded at 1×10^4 cells/well in a 96-well plate. Cells were incubated for 24 h (37°C, 5% CO_2) before treatment with varying final concentrations of DMSO [0, 1, 2, 4, and 8% (v/v)] diluted in tissue culture medium for 2 h, after which the DMSO was removed. Cells were next incubated with 150 ng/ml Anx-F for 30 min. After this time, the Anx-F was removed and cells were washed 3 times (10 mM HEPES, 150 mM sodium chloride, 2 mM calcium chloride, pH 7.4). Anx-F fluorescence was recorded in the same buffer using an Odyssey imaging system (Li-Cor Biosciences, Lincoln, NE, USA), and the results are expressed as fluorescence intensities normalized to controls (0% v/v DMSO).

Oxygen consumption measurement

The mitochondrial respiratory rates were measured using polarographic oxygen sensors in a 2-chamber Oroboros Oxygraph (Oxygraph 2-k; Oroboros Instruments, Obergurgl, Austria) with electromagnetic stirrers and thermostatically maintained at 37°C. The cells were grown to 100% confluency in a T75 flask. They were washed twice with warm PBS, trypsinized, and centrifuged for 2 min at 1000 *g*. The pellet of cells was gently resuspended in DMEM/HEPES [DMEM without sodium bicarbonate ($NaHCO_3$), including 5.5 mM glucose, and 20 mM HEPES] and kept in a 37°C water bath. Then, 2.5 ml of medium containing ~1 million cells was used for each experiment. The cells were transferred to a cuvette, which made contact with the O_2 membrane and different final concentrations of DMSO (to give final concentrations of 1, 2, and 4% v/v) were added. The system was then closed and, after it reached equilibrium, the levels of oxygen were recorded. Sequentially concentrations of the ATP-synthase specific inhibitor oligomycin (1 mg/ml) were given; coupled respiration was measured, followed by uncoupling with carbonylcyanide p-trifluoromethoxyphenylhydrazone (FCCP; 1 mM); uncoupled respiration was next assessed by inhibition at

complex III by antimycin A (1 mg/ml); and finally, ascorbate and *N,N,N′,N′*-tetramethyl-p-phenylenediamine (TMPD; 0.8 M) were added to determine the capacity of cytochrome *c* oxidase (complex IV), as described previously (34). The oxygen consumption was normalized to the number of cells in each cuvette and to the basal control levels.

Cell treatment with DMSO

RGC-5 cells were plated in a T75 flask (for Western blot extracts), on glass coverslips on a 12-well plate (for immunocytochemistry), on glass coverslips on a 6-well plate (for live cell imaging) or in 96-well plates (for the AlamarBlue assay) and then treated with different final concentrations of DMSO (0, 1, 2, 4, and 8% v/v) for 24 h, as in previous studies (2, 8, 9, 16).

In vitro cell viability and apoptosis assays

Terminal deoxynucleotidyl transferase dUTP nick end labeling (TUNEL), propidium iodide (PI), and Hoechst assays were used to assess the effects of DMSO on RGC-5 cells. For Hoechst staining, cells were grown to 80% confluency and separate wells were treated with DMSO at 0, 1, 2, 4, 8, and 10% final concentrations (2, 8, 9, 16). The cells were then fixed with 4% paraformaldehyde (PFA) for 30 min and stained with the cell permeable dye Hoechst 33342 (Molecular Probes, Eugene, OR, USA) at 5 μg/ml after a 5 min incubation at room temperature. Nuclear morphology was evaluated with a fluorescent microscope (Leica DM IRB; Leica Microsystems, Wetzlar, Germany) to allow assessment of apoptosis, which is characterized by bright staining and chromatin condensation (34). Condensed nuclei were counted using ImageJ (U.S. National Institutes of Health, Bethesda, MD, USA) and were presented as a percentage of the total number of cells in the field. For the simultaneous detection of apoptosis and necrosis, 3 markers were used. Cells were grown on glass coverslips to 80% confluence and treated with a 10 μM caspase-3 inhibitor in accordance with the manufacturer's protocol (Z-DEV-FMK, R&D Systems, Abingdon, UK; ref. 35) before addition DMSO at final concentrations of 1, 2, 4, and 8%. The cells were then washed twice with fresh cold PBS for 5 min each time, and incubated for 10 min on ice with both PI (Invitrogen) at 5 μg/ml and Hoechst 33342 (Molecular Probes, Eugene, OR, USA) at 10 μg/ml. The 5 min wash was repeated twice as before with fresh cold PBS, and the cells were fixed with 4% PFA in PBS for 30 min at 4°C. After being washed again, the cells were permeabilized with 0.2% Triton X-100 (Sigma-Aldrich, St. Louis, MO, USA). To distinguish fragmented nuclei, a TUNEL kit (DeadEnd Fluorometric TUNEL System; Promega, Madison, WI, USA) was used following the manufacturer's protocol.

The images were acquired on a Leica confocal scanning microscope SP2 (Leica Microsystems) using a ×40 oil objective lens coupled to a Kr/Ar laser (488 nm), an He/Ne laser (543 nm), and a blue diode (405 nm). The total number of cells, as well as the number of apoptotic and necrotic cells were counted using ImageJ 1.44p software. The percentage of apoptotic cells was calculated for each concentration in relation to the total number of cells and compared with the control. Cells stained with PI were colocalized with TUNEL, as described previously for final stage of apoptosis (36).

Western blot analysis of mitochondrial proteins

Cells were grown to 80% confluence and treated for 24 h in DMSO (1, 2 and 4%). For total extracts, cells were washed twice using fresh cold PBS (Sigma-Aldrich) and lysate using RIPA buffer (Sigma-Aldrich) for 10 min at 4°C on a plate shaker. Cells were dissociated using a P 1000 micropipette and stored at −20°C for further analysis.

For analysis of the mitochondrial, nuclear, and cytosolic fractions, cells were treated using a Qproteome Mitochondria Isolation kit according to the manufacturer's protocol (Qiagen, Hilden, Germany). The samples were stored at −20°C for further analysis.

The total protein content of samples was quantified using the bicinchoninic acid assay (BCA; Thermo Fisher Scientific, Rockford, IL, USA). Equal amounts of protein (20 or 40 μg) were loaded on 12% gels after denaturation with 4× concentrated sample buffer [30% v/v glycerol, 0.6 M dithiothreitol (DTT), 10% w/v sodium dodecyl sulfate (SDS), 715 mM Tris-HCl (pH 6.8), and 0.012% bromphenol blue], and were heat inactivated at 95°C for 5 min. The samples were separated by SDS–polyacrylamide gel electrophoresis (PAGE) and then electrotransferred to polyvinylidene difluoride (PVDF) membranes (GE HealthCare, Little Chalfont, UK). After blocking for 1 h at room temperature with 5% nonfat milk in Tris-buffered saline (20 mM Tris and 140 mM Nach, pH 7.6) containing 0.1% Tween 20 (TBS-T), the membranes were incubated overnight at 4°C with primary antibodies against apoptosis-inducing factor (AIF) 1:200 (SC-9416; Santa Cruz Biotechnology, Santa Cruz, CA, USA), Bax 1:200 (sc-6236; Santa Cruz Biotechnology), caspase-3 (BD Transduction Laboratory, Lexington, KY, USA), cleaved caspase-3 (Asp175, Cell Signaling Technology), and poly-(ADP-ribose)-polymerase (PARP) 1:500 (Cell Signaling Technology, Danvers, MA, USA). After being washed 3 times (15 min with TBS-T), the membranes were incubated for 2 h at room temperature with their respective alkaline phosphatase-linked secondary antibody (Cell Signaling Technology and DAKO, Carpinteria, CA, USA) in TBS-T containing 5% nonfat milk. The membranes were then washed 3 times (15 min in TBS-T), and protein bands were revealed with enhanced chemiluminescent substrate (ECL; GE HealthCare). The membranes were then reprobed and tested for α-tubulin (DM1A; Cell Signaling Technology) or VDAC (Cell Signaling Technology) immunoreactivity as loading controls.

Live cell imaging using Fluo-4

Live cell imaging was performed using a Zeiss LSM uv-vis 510 META (Carl Zeiss, Oberkochen, Germany). Experiments were carried out at 37°C. The cells were washed twice with PBS, and growth medium was replaced by HEPES-buffered saline solution (156 mM NaCl, 3 mM KCl, 2 mM $MgSO_4$, 1.25 mM KH_2PO_4, 2 mM $CaCl_2$, 10 mM glucose, and 10 mM HEPES, pH 7.35). Fluo-4 AM was loaded 45 min before the beginning of the experiment to final concentrations of 2 μM followed by washing. Fluo-4 fluorescence was excited using a Kr/Ar laser at 488 nm. Images were acquired every 15 min for 2 h and were later analyzed using ImageJ software.

Measurement of NADH autofluorescence

As before, live cell imaging was performed using a Zeiss uv-vis LSM 510 META (Zeiss). Experiments were carried out at 37°C. The cells were washed twice with PBS, and growth medium was replaced by HEPES-buffered saline solution as described above. NADH autofluorescence was excited at 351 nm and was measured using bandpass filter between 435 and 485 nm every 2 min for 20 min and quantified using ImageJ software.

AlamarBlue assay

Cell viability using a PARP inhibitor or calpain inhibitor at the same time as DMSO was assessed using the AlamarBlue (Invitrogen) viability assay, following preliminary experiments to identify the most appropriate concentrations. RGC-5 cells were plated in a 96-well plate at 4000 cell/ml, and the cells were pretreated for 1 h with either a PARP inhibitor (10 μM PARP inhibitor III, DPQ; Merck Millipore, Nottingham, UK) or calpain inhibitor (1 μM calpeptine; Merck Millipore). DMSO (2%) was added to the cells with the inhibitors and incubated for 24 h. Filtered AlamarBlue solution (10 μl) was added to each 100 μl well plate and incubated for 2.30 h according to manufacturer's protocol. The fluorescence was read at 585 nm with results presented as a percentage of the control.

Statistical analysis

Graphical data are represented as mean ± SEM values. Statistical comparisons between different concentrations of DMSO animals and controls were performed using the 1-way ANOVA followed by Dunnett or Bonferroni *post hoc* test using GraphPad Prism (GraphPad, San Diego, CA, USA). Differences were considered significant at values of $P < 0.05$.

RESULTS

DMSO is toxic to RGCs *in vivo*

To evaluate the effects of DMSO on rat RGCs *in vivo*, injections (5 μl) of various stock concentrations of DMSO (0, 1, 2, 4, 8, 10, 15, and 25% v/v) were administered IVT to Dark Agouti rats with Anx-F. Dosing of high stock concentrations of DMSO (≥10% v/v) resulted in lens toxicity, causing opacity and poor visualization of the retina. DMSO was found to be toxic at all stock concentrations dosed <10% (v/v; vitreal concentration 0.1, 0.2, 0.4, 0.7, 0.9, and 1.4% v/v) 2 h after intravitreal administration, inducing significant ($P<0.01$, 1-way ANOVA) RGC apoptosis as detected by Anx-F-positive cells [**Fig. 1**, white spots indicate apoptosing cells on the retina, present after dosing DMSO stock concentrations of 1% (*B*), 2% (*C*), 4% (*D*), and 8% v/v (*E*)]. This occurred in a dose-dependent manner, with RGC apoptosis increasing by 585, 717, 877, and 1620% compared with control with dosing 1, 2, 4, and 8% (v/v) stock DMSO concentrations respectively (Fig. 1*F*).

DMSO is toxic to RGCs *in vitro*

Having established that low concentrations of DMSO were toxic in the retina *in vivo*, we next investigated the toxicity of DMSO *in vitro*. RGC-5 viability and apoptosis were determined using Hoechst 33342 nucleic staining following a 24 h treatment with 1, 2, 4, 8, or 10% (v/v) DMSO. Hoechst 33342 staining is dull in normal cells but much stronger when the chromatin is condensed in apoptotic cells, allowing for both total and pyknotic cell

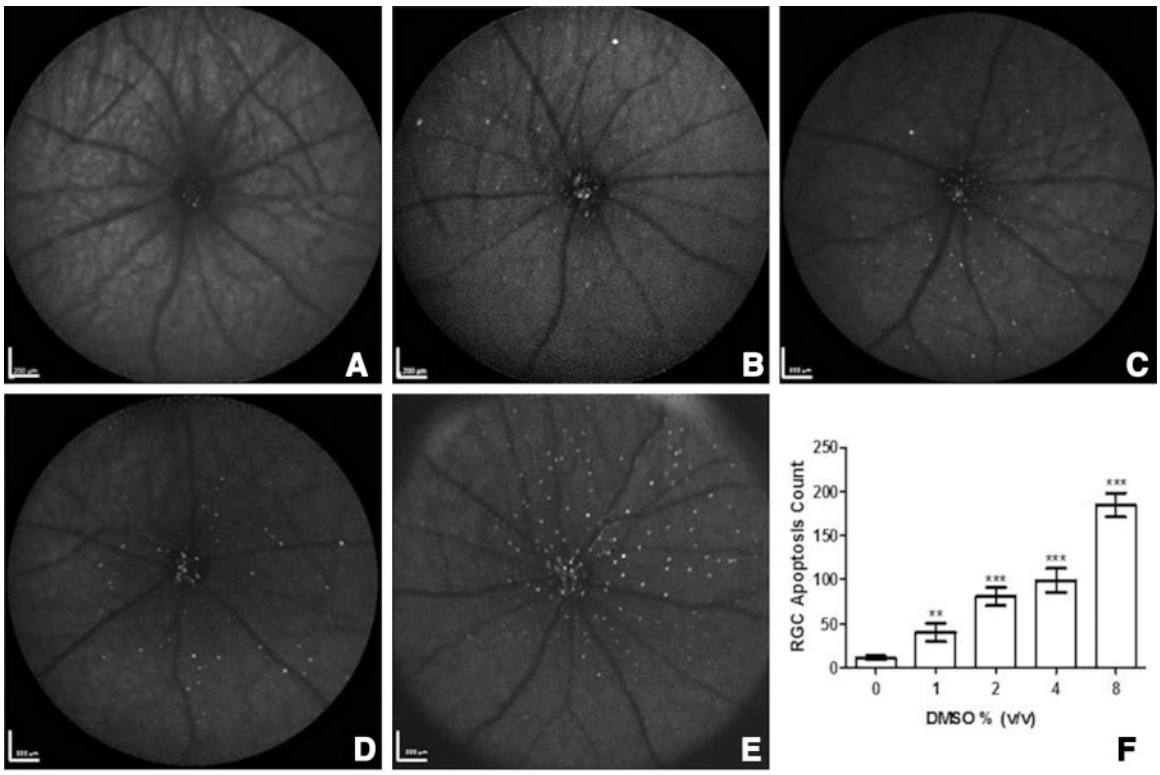

Figure 1. DMSO toxicity *in vivo*: effects on RGC apoptosis. *In vivo* DARC images obtained using an HRA Spectralis (Heidelberg Engineering), show the effects of 5 μl of intravitreally administered DMSO at indicated stock concentrations of 0, 1, 2, 4, or 8% (v/v) on RGC apoptosis 2 h following intravitreal injection of fluorescently labeled annexin V (Anx-F). White spots represent apoptotic RGCs labeled by Anx-F. *A–E*) Wide-angle *in vivo* retinal images: PBS control (*A*), 1% DMSO (v/v; *B*), 2% DMSO (v/v; *C*), 4% DMSO (v/v; *D*), and 8% DMSO (v/v; *E*). Scale bars = 200 μm. *F*) Statistical analysis of the number of Anx-F-positive cells after intravitreal injection of PBS or DMSO. Error bars represent SEM. $*P < 0.05$; $**P < 0.01$; $***P < 0.001$.

counts to be made. DMSO was found to induce cell loss and apoptosis in a dose dependent manner (**Fig. 2*A–H***). The total number of cells fell by 24, 50, 70, 92, and 98% respectively, with significance at 1% ($P<0.05$) and at concentrations ≥2% DMSO ($P<0.01$) compared with control (Fig. 2*A*). Similarly, the number of pyknotic nuclei increased by 100, 550, 1725, and 2025% (percentage of total cells) compared with control (2, 4, 8 and 10% DMSO, respectively), with a significant increase noted at 1 ($P<0.05$), 2 ($P<0.01$), and 4% ($P<0.001$, 1-way ANOVA) DMSO (Fig. 2*B*). These effects are clearly seen in the representative Hoechst 33342 images at DMSO final concentrations of 0 (Fig. 2*C*), 1% (Fig. 2*D*), 2% (Fig. 2*E*), 4% (Fig. 2*F*), 8% (Fig. 2*G*), and 10% DMSO (Fig. 2*H*).

Cell viability was further assessed using an 3-(4,5-dimethylthiazol-2-yl)-2,5-diphenyltetrazolium bromide (MTT) assay after 24 h treatment with 1, 2, 4, 8, and

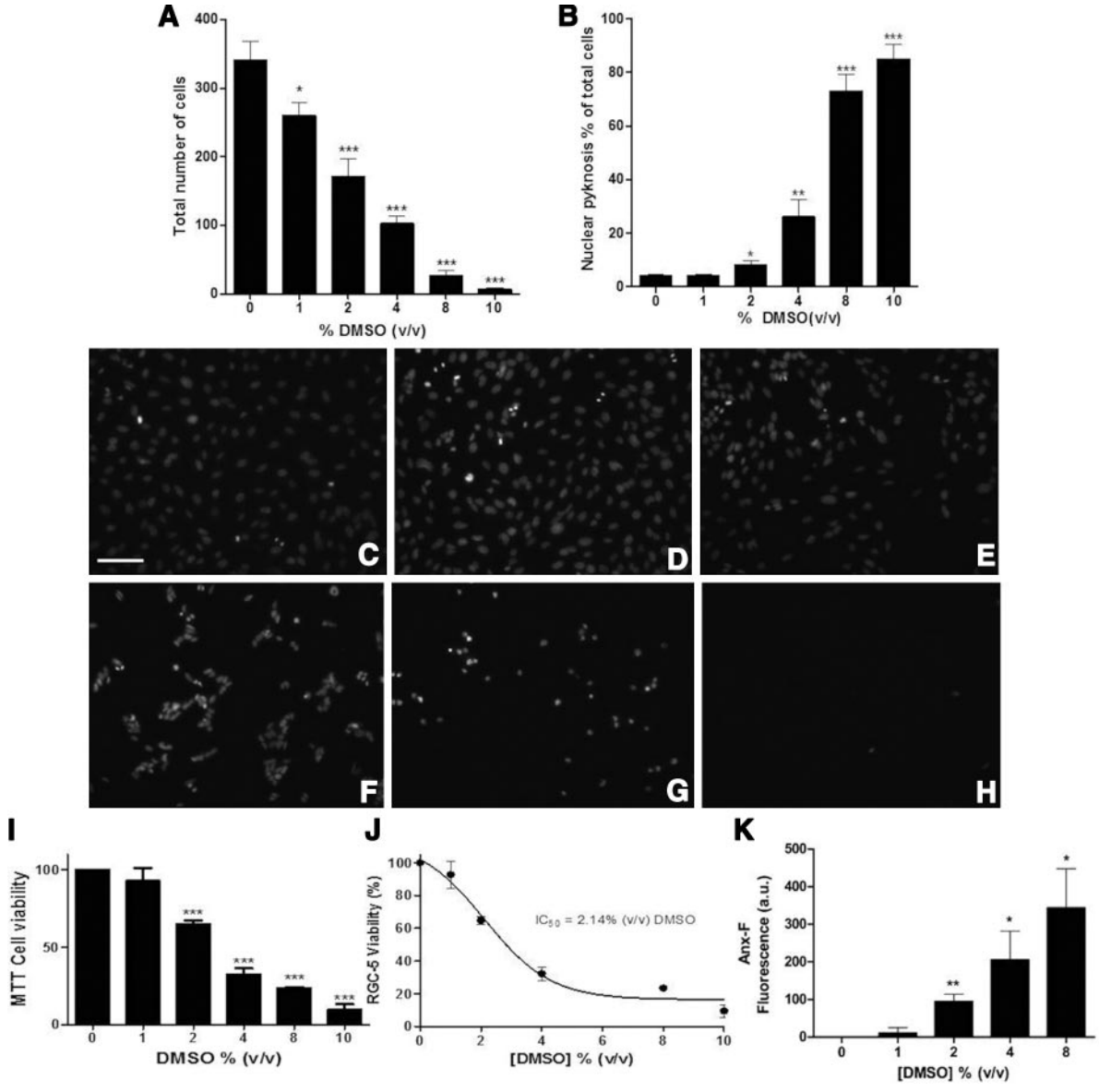

Figure 2. DMSO toxicity *in vitro*: effects on RGC viability and apoptosis. Effects of DMSO after 24 h treatment at final concentrations of 0, 1, 2, 4, 8, and 10%. DMSO increases chromatin condensation and decreases total cell count in a dose-dependent manner. Cell viability was determined by nucleic morphology with Hoechst 33342 nucleic staining. Total cells and apoptotic cells per field were counted using ImageJ for each concentration. *A*) Total number of cells per image at $t = 24$ h. *B*) Number of cells with pyknotic nuclei, represented as a percentage of total cells. *C–H*) Representative images: control (*C*), 1% DMSO (*D*), 2% DMSO (*E*), 4% DMSO (*F*), 8% DMSO (*G*), and 10% DMSO (*H*). Scale bar = 100 μm. *I*) MTT assay was performed after 24 h treatment of RGC-5 cells with different final concentrations of DMSO (0, 1, 2, 4, 8, and 10% v/v). A significant decrease in cell viability was observed with final concentrations >1% DMSO (v/v). *J*) IC_{50} occurs at 2.14% (v/v) DMSO). *K*) After 2 h treatment, (0, 1, 2, 4, and 8% v/v DMSO), RGC-5 cells exhibited a significant increase in phosphatidylserine externalization reported after 30 min incubation with the fluorescent conjugated annexin V (Anx-F, $n=3$, means±SEM). Statistical analysis using 1-way ANOVA followed by Dunnett's multiple comparison test. Error bars represent SEM. $^*P < 0.05$; $^{**}P < 0.01$; $^{***}P < 0.001$.

10% (v/v) DMSO. A decrease in cell viability was observed with final concentrations >1% DMSO ($P<0.001$, 1-way ANOVA), being 35, 68, 76, and 90.5%, respectively for 2, 4, 8, and 10% DMSO (Fig. 2*I*). The IC_{50} was also calculated after 24 h and was found to be at 2.14% DMSO (Fig. 2*J*).

As apoptosis is associated with phosphatidylserine (PS) externalization, we next investigated whether DMSO induced PS externalization *in vitro*. RGC-5 cells were treated with varying final concentrations of DMSO (0, 1, 2, 4, and 8%) for 2 h and incubated with Anx-F for 30 min. Treatment of RGC-5 cells with final concentrations of DMSO ≥2% (v/v) caused significant ($P<0.05$, *t* test) dose-dependent phosphatidylserine externalization compared with untreated controls (Fig. 2*K*).

DMSO inhibits mitochondrial oxygen consumption and increases intracellular calcium concentration

Mitochondria play a crucial role in the control of apoptotic events. Having established that DMSO induces cell death, we next investigated whether this was related to changes in mitochondrial function. Basal cellular oxygen consumption by the RGC-5 cells in suspension was significantly reduced following addition of 1, 2, and 4% DMSO ($P<0.001$; **Fig. 3*A***). Inhibition of oxidative phosphorylation by oligomycin decreased oxygen consumption, indicating the fraction of basal respiration attributable to ATP synthase activity at 2 and 4% DMSO (Fig. 3*B*). Application of the uncoupler FCCP increases oxygen consumption to reveal the

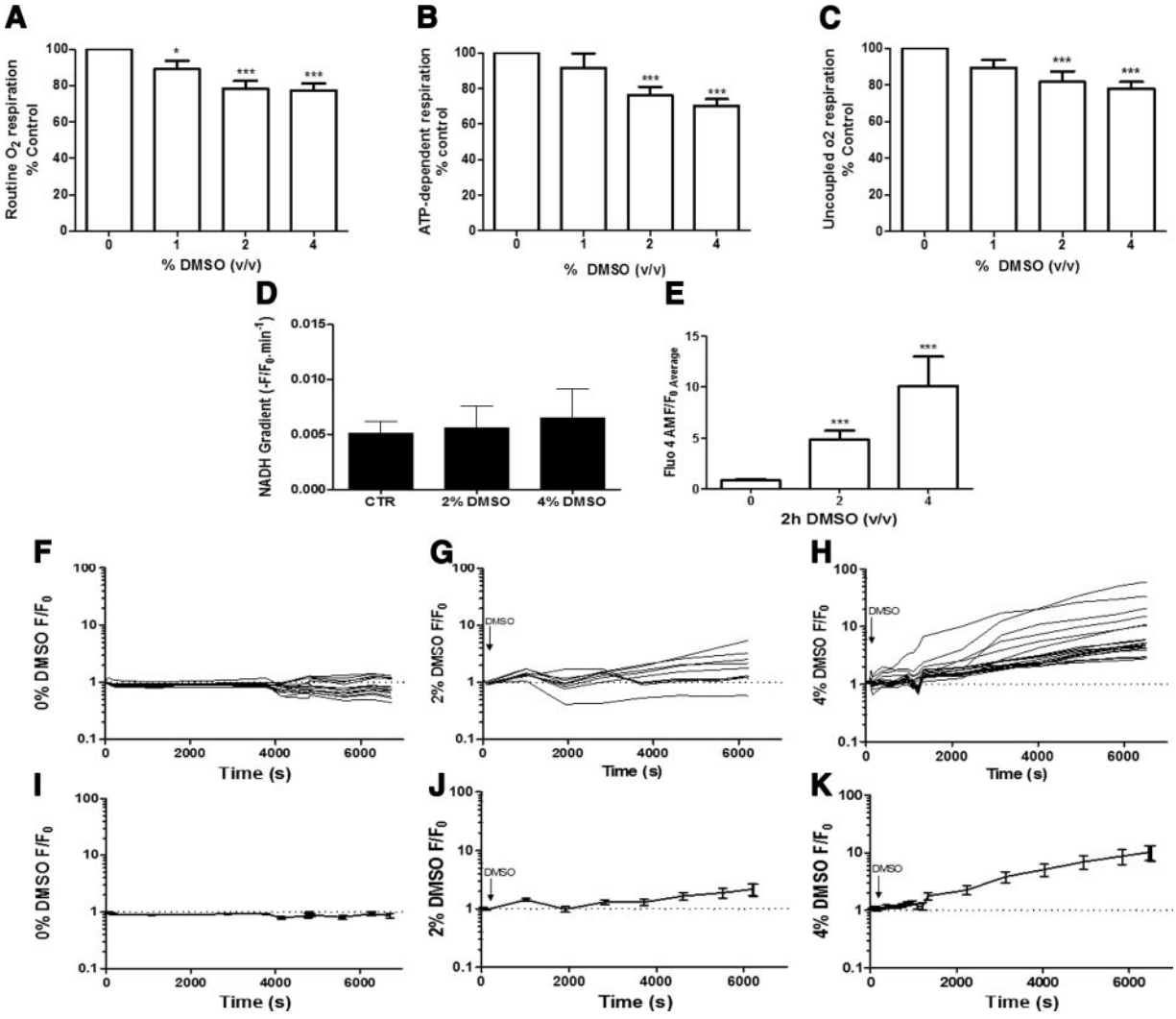

Figure 3. Effects of DMSO-induced apoptosis involve mitochondrial dysfunction. *A*) Oxygen consumption was measured in RGC-5 cells. There is significant inhibition of mitochondrial respiration at final concentrations of 1, 2, and 4% DMSO. $*P < 0.05$; $***P < 0.001$. *B*) DMSO was found to significantly decrease ATP-dependent respiration, at both 2 and 4%. $***P < 0.001$. *C*) Moreover, addition of the uncoupler FCCP induced a decrease in respiration at both 2 and 4% DMSO. $***P < 0.001$. *D*) NADH levels were evaluated using live cell imaging for a period of 20 min. Graph represents the gradient of each curve that was shown not to be significant with 2 and 4% DMSO (v/v). *E–K*) Fluo-4 AM analysis assessing intracellular calcium was performed. Average of F/F_o single cells at the end point of the experiment for each concentration (2 h), shows that DMSO at both 2 and 4% final concentrations causes a significant increase in $[Ca^{2+}]_c$ in RGC-5 cells (*E*). This change is clearly shown in the raw data of calcium levels with single-cell (*F–H*) and average (*I–K*) analysis of the raw data for control (*F, I*), 2% (*G, J*), and 4% (*H, K*) DMSO F/F_o, respectively. Error bars represent SEM. $***P < 0.001$; *t* test analysis.

maximal respiratory capacity. This measure was significantly decreased at 2 and 4% DMSO compared with control ($P<0.001$; Fig. 3*C*), consistent with damage to the respiratory chain or decreased substrate availability. Finally, antimycin A, a complex III inhibitor, was added demonstrating that the oxygen consumption was due to mitochondria respiration. The levels of NADH were next investigated to assess the redox state of the mitochondrial NAD system by recording changes in NADH fluorescence. The NADH pool is expected to become more reduced if respiration is inhibited, while the cellular NAD pool becomes depleted by PARP activation. NADH levels were not significantly affected by the addition of 2 and 4% (v/v) DMSO (Fig. 3*D*), suggesting that the decreased respiratory rates were not secondary to substrate depletion. Next, intracellular calcium concentrations ($[Ca^{2+}]_c$) were investigated using Fluo-4. Changes in $[Ca^{2+}]_c$ were quantified over a period of 2 h following exposure to DMSO (Fig. 3*E*) and showed a progressive and significant increase at both 2 and 4% (v/v) final concentrations ($P<0.001$) compared with control. Both single cell (Fig. 3*F–H*) and average traces (Fig. 3*I–K*) clearly showing a progressive increase in intracellular $[Ca^{2+}]_c$ exposed to 2 and 4% DMSO over time (Fig. 3*F–K*).

To assess the involvement of the mPTP in DMSO-induced cell death, we also tested whether the mPTP inhibitor cyclosporine A (CsA) had an impact on DMSO-induced cell death. CsA did not decrease cell death in any of the DMSO final concentrations tested indicating that DMSO-induced cell death is mPTP independent (data not shown).

Apoptosis induced by DMSO is caspase-3 independent

Having established that DMSO induces apoptosis at low concentrations, we next investigated whether this involved caspase-3. RGC-5 cells were incubated with the caspase-3 inhibitor Z-DEVD-fmk (10 μM) and DMSO (0, 1, 2, 4, and 8% v/v) for 24 h. Apoptosis and cell death were determined using Hoechst, TUNEL, and PI staining (**Fig. 4*A–D***). Firstly, the presence of the caspase-3 inhibitor had no effect on RGC-5 loss (Fig. 4*A*); cell viability still decreased with increasing final concentrations of DMSO, as assessed using Hoechst (Fig. 4*A*, *D*). Similarly, Z-DEVD-fmk did not influence the number of TUNEL-positive cells, and increased apoptosis was still associated with increasing final concentrations of DMSO (Fig. 4*B*, *D*). Finally, the number of PI-positive cells increased with increasing DMSO final concentrations, until 8% DMSO when the majority of cells were stained with PI, with no effect by caspase-3 inhibition (Fig. 4*C*, *D*). The findings were further supported by Western blot analysis, which showed no caspase-3 activity in RGCs at any of the DMSO final concentrations tested (Fig. 4*E*), strongly suggesting that the pathway by which DMSO triggers cell death is caspase-3 independent.

DMSO induces cell death by nuclear translocation of AIF and translocation of Bax to mitochondria

To determine the pathway by which DMSO induces cell death, concentrations of the proapoptotic proteins AIF and Bax were evaluated in mitochondrial, nuclear, and cytosolic fractions of RGC-5 cells treated with DMSO. Western blot analysis showed that after 24 h treatment, there was a gradual decline in the levels of mitochondrial AIF (**Fig. 5*A, B***) with increasing final concentrations of DMSO, while a concomitant increase in nuclear AIF (Fig. 5*A*, *C*) was observed at equivalent concentrations. This is in accordance with AIF translocation from the mitochondria to the nucleus during apoptosis. VDAC and α-tubulin were used as loading controls for the mitochondrial and cytosolic fractions, respectively (Fig. 5*A*). Immunocytochemistry analysis was performed using an AIF antibody after 24 h exposure to different final concentrations of DMSO (Fig. 5*D*). From concentrations >1% DMSO (v/v), more AIF is seen in the nucleus, as demonstrated by the colocalization plots with AIF and nuclear staining (Hoechst; Fig. 5*D*). This is in keeping with AIF translocation from the mitochondria to the nucleus, as revealed by Western blots analysis in Fig. 5*A–C*. The level of proapoptotic Bax was evaluated similarly to AIF using Western blots. Mitochondrial Bax (Fig. 5*A*, *E*) was increased at 2 and 4% DMSO, and this was paralleled by a corresponding decrease in cytosolic Bax at the same concentrations (Fig. 5*A*, *F*). This is in accordance with Bax oligomerization at the mitochondrial level. These data strongly support the proposition that DMSO induces AIF translocation from mitochondria to the nucleus through Bax-induced mitochondria permeabilization.

DMSO causes PARP-1 activation

As AIF translocation has been associated with the activation of PARP-1 (36, 37), we next assessed the levels of PARP-1 expression in whole-cell extracts of RGC-5 cells by Western blot after 24 h after treatment with DMSO (0, 1, 2, 4, and 8% v/v). The anti-PARP-1 antibody used detects both the full-length (116 kDa) and cleaved (activated) form (86 kDa) (**Fig. 6*A***). We detected cleaved PARP-1 at 2, 4, and 8% v/v DMSO final concentrations, and this was found to be statistically significant compared with control, 2% ($P<0.05$), and >4% ($P<0.001$; Fig. 6*B*). This suggests that PARP-1 activation is involved in the pathway by which DMSO induces cell death.

To further evaluate the involvement of PARP and calpains on the proposed pathway, we used PARP and calpain inhibitors to investigate DMSO-induced cell death with the AlamarBlue cell viability assay. Both the PARP inhibitor ($P<0.001$; Fig. 6*C*) and calpain inhibitor ($P<0.05$; Fig. 6*D*), significantly inhibited DMSO-induced cell death with 1 h pretreatment and 24 h treatment of 2% DMSO. These results strongly suggest the involvement of both PARP-1 and calpain in DMSO-induced cell death.

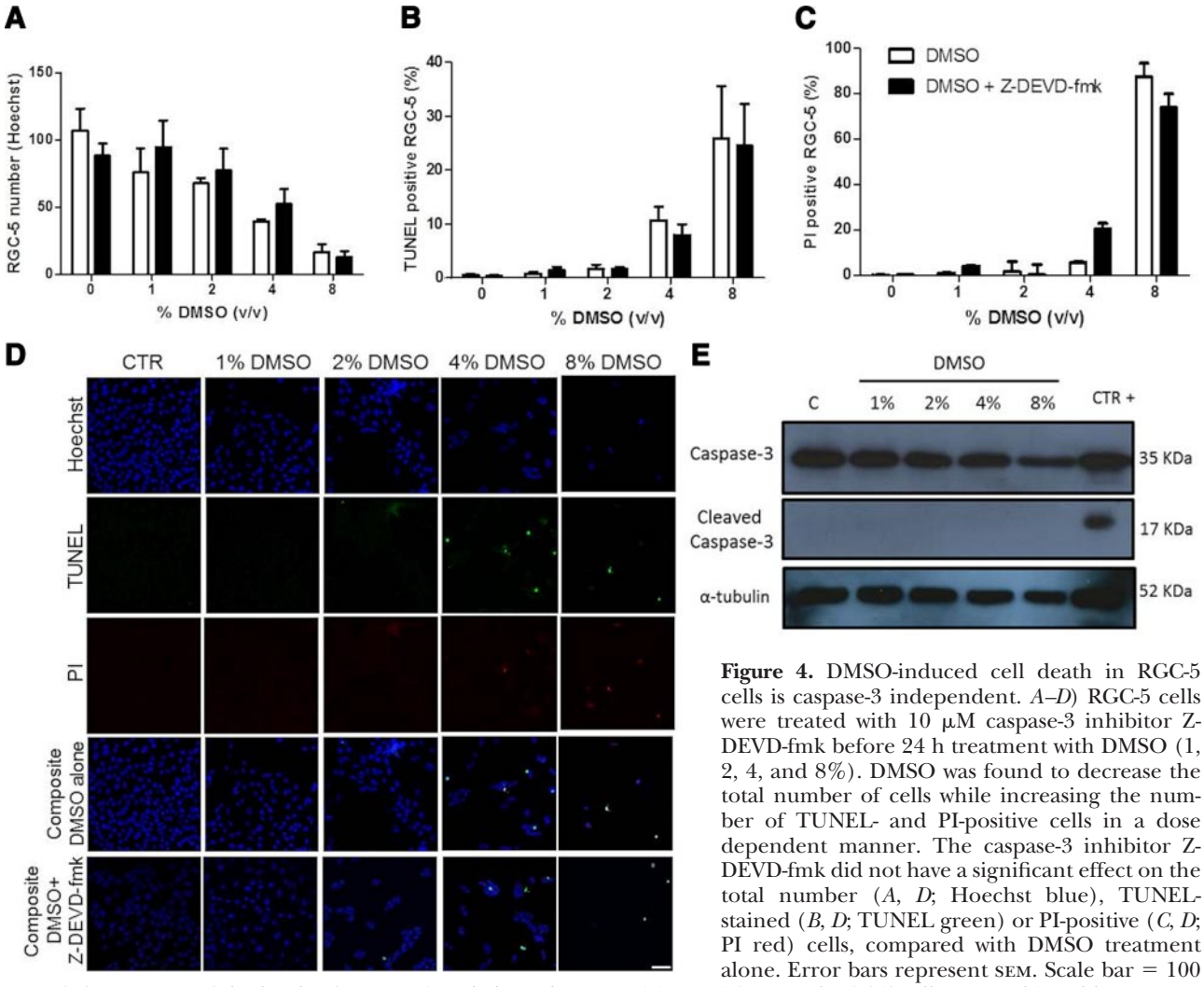

Figure 4. DMSO-induced cell death in RGC-5 cells is caspase-3 independent. *A–D*) RGC-5 cells were treated with 10 μM caspase-3 inhibitor Z-DEVD-fmk before 24 h treatment with DMSO (1, 2, 4, and 8%). DMSO was found to decrease the total number of cells while increasing the number of TUNEL- and PI-positive cells in a dose dependent manner. The caspase-3 inhibitor Z-DEVD-fmk did not have a significant effect on the total number (*A*, *D*; Hoechst blue), TUNEL-stained (*B*, *D*; TUNEL green) or PI-positive (*C*, *D*; PI red) cells, compared with DMSO treatment alone. Error bars represent SEM. Scale bar = 100 μm. *E*) Assessment of the levels of caspase-3 and cleaved caspase-3 in DMSO-treated RGC-5 cells were achieved by Western blot. No detection of activated caspase-3 was seen at any of the DMSO final concentrations (1, 2, 4, and 8%) tested. A positive control and a loading control (α-tubulin) were used.

DISCUSSION

Our findings have shown that final concentrations of DMSO as low as 0.1% (v/v) are toxic *in vivo* (1, 2, 4, and 8% v/v stock; 5 μl injected volume) causing significant retinal apoptosis. This is different to what has been previously reported, and the widely accepted belief that DMSO is well tolerated at concentrations <10% (8, 16–19). In previous intravitreal *in vivo* studies (2–4, 7, 10–15, 19, 39, 40), the stock concentrations of DMSO administered are reported, although we have also quantified corresponding final vitreous concentration of 0.1, 0.2, 0.4, 0.7, 0.9, 1.4, and 2.3% (v/v) based on the DA rat vitreous volume of 55 μl. DMSO is also toxic to RGC-5 cells *in vitro,* as demonstrated using fluorescently labeled annexin V, TUNEL, PI, MTT, and Hoechst as neuronal cell viability assays. The effective concentrations of DMSO required to induce toxicity were greater *in vitro* than *in vivo.* This can be readily explained as it is well documented that cell lines are more resistant to insults than primary cell cultures (41). High concentrations of DMSO (>10% v/v) have previously been shown to induce toxicity (5, 6, 40) through plasma membrane pore formation (23, 24). In the present study, we describe a new mechanism by which DMSO induces neuronal death at significantly lower concentrations than previous reported. Cell death is induced through AIF translocation to the nucleus and stimulation of a caspase-3 independent pathway of apoptosis, involving PARP activation. Our proposed pathway (**Fig. 7**) is initiated by inhibition of mitochondrial respiration with elevation of intracellular calcium concentration. This is followed by phosphatidylserine externalization on the cell membrane. Next, Bax oligomerization induces mitochondrial permeabilization, which in turn is followed by AIF translocation, PARP activation, and, finally, cell death.

DMSO is used widely in the eye as a vehicle control (8, 9, 12, 14–19, 42), and there are several studies claiming no adverse effects (43–45). It has been used topically (1–50% v/v; refs. 12, 13), subconjunctivally (80–100% v/v; ref. 14), and IVT (up to 100% v/v; refs. 16, 18), but most often, its absolute concentration is not

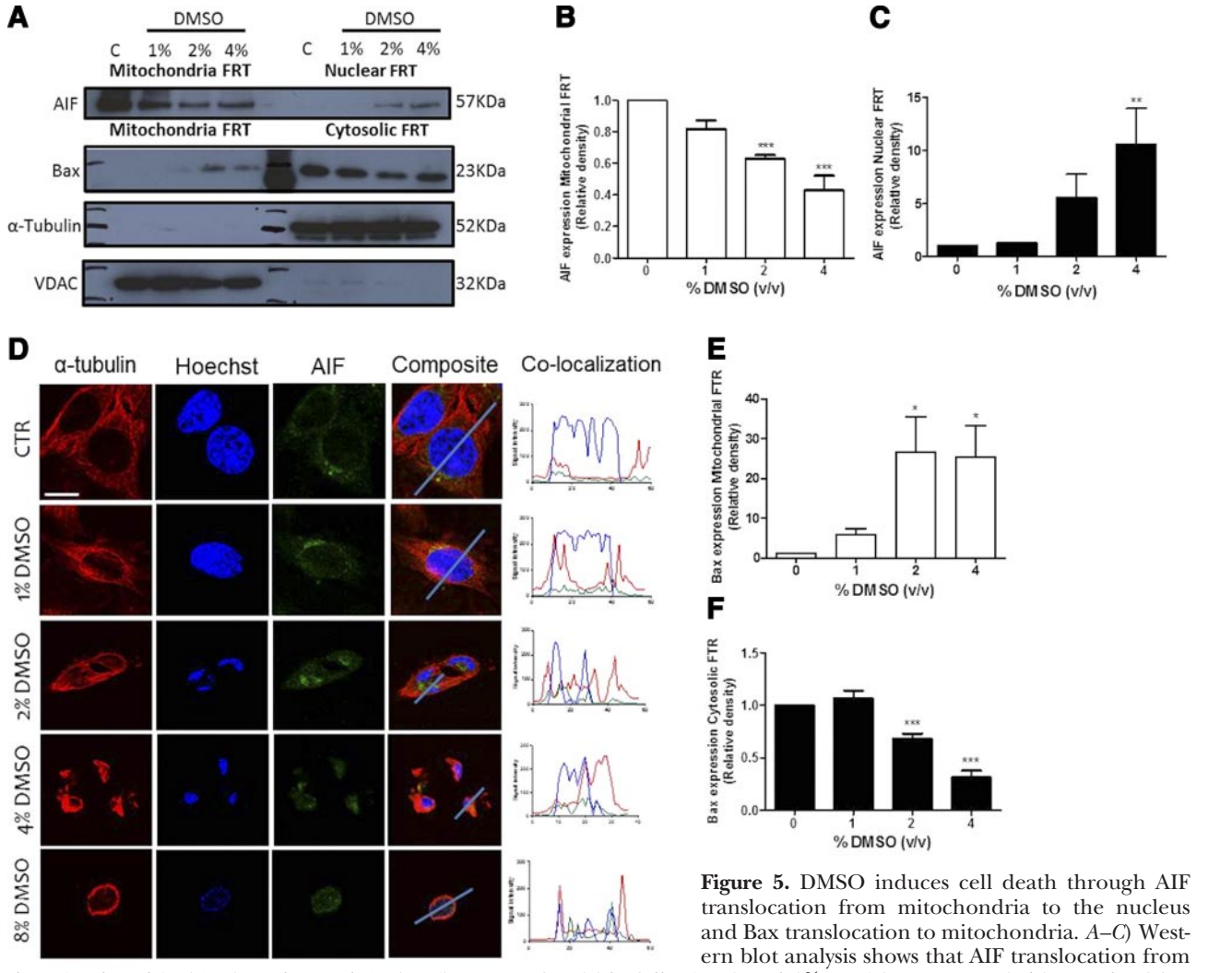

Figure 5. DMSO induces cell death through AIF translocation from mitochondria to the nucleus and Bax translocation to mitochondria. *A–C*) Western blot analysis shows that AIF translocation from the mitochondria (*A, B*) to the nucleus (*A, C*) occurs after 24 h, following 2 and 4% DMSO treatment (v/v). Levels of AIF were decreased in mitochondria fractions with increasing DMSO final concentrations (*A, B*), while increasing AIF in nuclear fractions (*A, C*). *D*) Immunocytochemistry images show immunoreactivity against AIF (green), α-tubulin (red), and Hoechst (blue) at different final concentrations of DMSO after 24 h treatment. Scale bar = 20 μm. *E, F*) Signal intensity profiles show colocalization of AIF and Hoechst at 2, 4 and 8% DMSO (*F*), confirming concentration-dependent AIF translocation to nucleus. Similarly, the levels of Bax change: with increasing DMSO final concentrations, levels of Bax increased in mitochondrial fractions (*A, E*) while decreasing in cytosolic fractions (*A, F*). VDAC and α-tubulin were used as loading controls for the mitochondrial (*E*) and cytosolic (*F*) fractions, respectively. Error bars represent SEM. $^{*}P < 0.05$; $^{**}P < 0.01$; $^{***}P < 0.001$.

reported (8, 9, 15–17). There is some functional, although no structural evidence that retinal toxicity is induced by low concentrations (0.6–8% v/v) of DMSO, but this study was based only on electrophysiology data (46).

However, DMSO has been reported to induce apoptosis *in vivo* elsewhere in the body. After intraperitoneal application to mice, apoptosis was reported in the developing central nervous system at 10 ml/kg of DMSO (100% v/v; ref. 6). Moreover, intraperitoneal injections of 4 ml/kg of DMSO (10% v/v) have been found to induce Tau hyperphosphorylation in the brains of C57/129 mice (5). We believe our data suggest that DMSO could be used as a new, inexpensive model for retinal neuron cell death and neurodegeneration *in vivo*, with the opportunity of providing a rapid assessment of neuroprotective strategies.

In vitro, DMSO is reported to induce apoptosis at concentrations >10% (v/v), due to plasma membrane pore formation (23, 24). Although rare, there are a few reports of effects of DMSO at low concentrations causing toxicity in cell types other than neurons. In EL-4 lymphoma cells, for example, 2.5% (v/v) DMSO was reported to induce apoptosis through a mitochondrial-mediated, caspase-3- and caspase-9-dependent pathway, associated with down-regulation of Bcl-2, loss of mitochondrial membrane potential, and release of cytochrome *c* from the mitochondria to the cytoplasm (25). Elsewhere, exposure of U937 (monocytes) to 1% (v/v) DMSO for 48 h was reported to have no effect on apoptotic signaling proteins {Bcl-2, Fas-associated protein with death domain (FADD), caspase-3 and caspase-8, inhibitor of apoptosis proteins (IAPs), or cellular FLICE-inhibitory protein [cFLIP(L)]}. Finally,

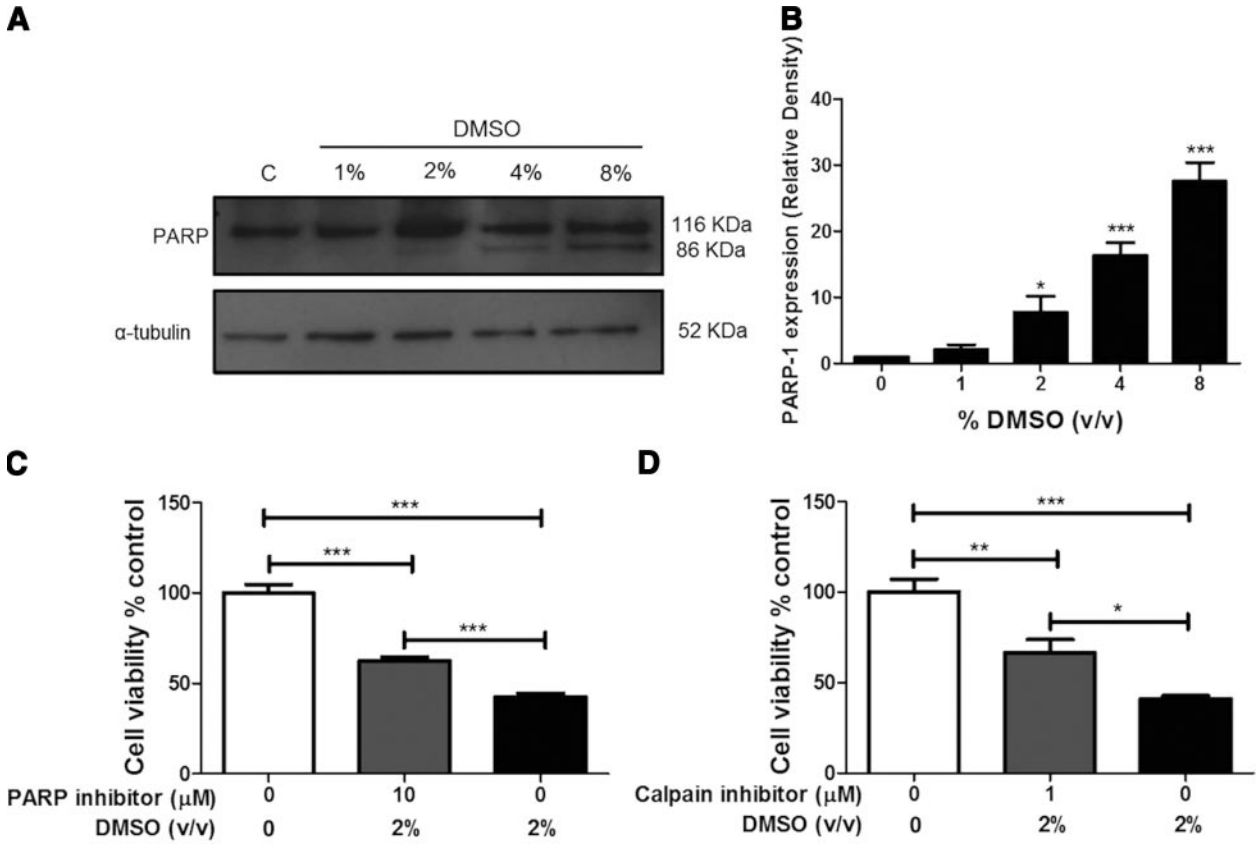

Figure 6. DMSO induces PARP activation. *A*) Western blot analysis shows PARP-1 activation at 2, 4, and 8% DMSO after 24 h treatment. α-Tubulin was used as the loading control. *B*) Statistical analysis identified a significant increase in the levels of PARP-1 activation after exposure of RGC-5 cells to 2, 4, and 8% v/v DMSO. *C, D*) Cell viability assay using AlamarBlue was performed after pretreatment of cells with PARP (*C*) or calpain (*D*) inhibitors with 2% DMSO compared with 2% DMSO alone. Statistical analysis shows a significant reduction in cell death with PARP ($P<0.001$; *C*) or calpain ($P<0.05$; *D*) inhibitor treatments, although levels did not return to control ($P<0.001$). Error bars represent SEM. $*P < 0.05$; $**P < 0.01$; $***P < 0.001$ *vs.* controls.

treatment of U937 cells in this way was found to lead to an increased sensitivity to receptor-mediated apoptosis (47). In ocular tissues, 48 h incubation with 1% (v/v) DMSO to human lens epithelial cells has been reported to decrease cell viability (MTT assay) and increase cellular apoptosis (TUNEL assay; ref. 48). In ARPE 19 (human retinal pigment epithelial cell line), there is a significant increase in caspase-3/7 activity after 24 h treatment with 1 mg/ml and 0.5 mg/ml DMSO (0.11 and 0.055% v/v, respectively) although the same was not observed on r28 (retinal precursor cell line; ref. 49).

The present study suggests that DMSO induces apoptosis *via* inhibiting mitochondrial respiration and increasing intracellular calcium. DMSO crosses biological membranes (50) and has been reported to induce apoptosis through mitochondrial depolarization as visualized using JC-1 (25). The results of the present study suggest a similar process occurs in RGCs, as inhibition of mitochondrial respiration was observed after 1, 2, and 4% (v/v) DMSO application (Fig. 3). Mitochondria play a crucial role in many models of cell death and determine the irreversibility of cell injury (22). However, there are several issues to consider with regard to the effects of DMSO on mitochondrial respiration. Analysis of the fraction of respiration that is ATP dependent revealed a significant decrease ($P<0.001$) in this parameter at 2 and 4% (v/v) DMSO, suggesting an effect of DMSO on ATP synthase activity. Measurement of maximal mitochondrial respiration was provided by FCCP, which is an uncoupler of the electron transport chain and oxidative phosphorylation. Both 2 and 4% DMSO reduced maximal respiratory capacity in response to uncoupler, providing further evidence of a direct effect of DMSO on the mitochondrial membrane. This observation is in broad agreement with previous observations in intact and permeabilized neurons (51). We found that after DMSO application mitochondrial respiration was decreased while PARP was activated. The association between PARP activation and inhibition of mitochondrial respiration is well documented, and inhibition of mitochondria respiration is reported to precede or proceed PARP activation (52, 53). PARP activation and NAD^+ depletion can cause decreased mitochondrial respiration and would reduce both basal and maximal respiratory capacity in conjunction with a decrease in NADH. Our results, however, did not show any significant change in NADH, suggesting that changes in mitochondrial respiration induced by DMSO precede PARP activation. Moreover,

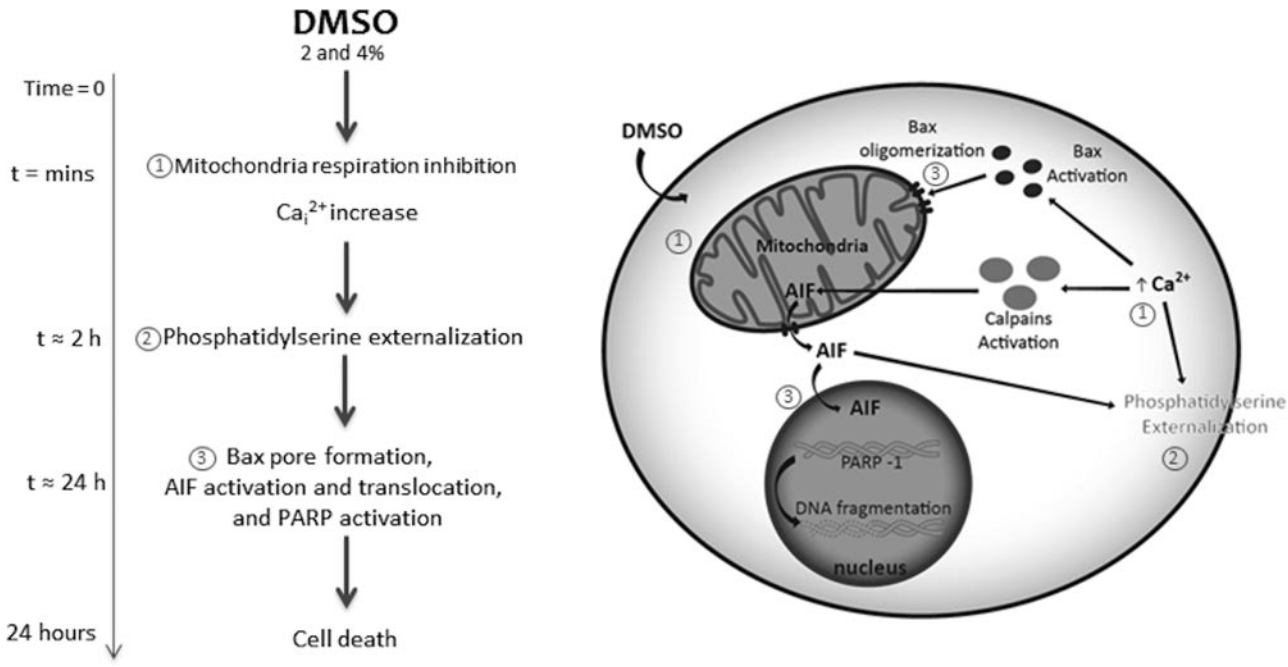

Figure 7. Proposed pathway for the induction of neuronal cell death in the eye by low doses of DMSO. DMSO (2–4% v/v) inhibits mitochondrial respiration and stimulates intracellular calcium transients. This leads to phosphatidylserine externalization and the earliest stages of apoptosis. Bax oligomerization induces mitochondrial permeabilization, and AIF activation and translocation. Apoptosis continues through PARP activation resulting in cell death. Timeline shown is based on *in vitro* results.

changes in the lipid content of the mitochondrial membrane are reported to affect mitochondrial respiration, and as DMSO has been suggested to interfere with lipid structure, this could provide an alternative explanation for the effects observed in the present study. Furthermore, on analysis of complex IV activity, our results indicated that the inhibitory effects observed were not due to complex IV inhibition. As all 3 mitochondrial parameters measured (basal respiration, ATP dependent, and FCCP) decreased in the presence of DMSO, this implies mitochondrial function is directly impaired on addition of DMSO. An increase in intracellular calcium was observed after DMSO application (Fig. 7). DMSO-induced cytoplasmic calcium influx has previously been reported in isolated Balanus eburneus photoreceptors after application of 5% (v/v) of DMSO, which is in accordance with our results (54). Calcium cell dysregulation is associated with cell death particularly in muscle and neuronal cells (55). While increased intracellular calcium leads to mitochondrial Ca^{2+} uptake, up-regulation of the TCA cycle, and increased oxidative phosphorylation (55, 56), Ca^{2+} overload may induce formation of the mitochondrial permeability transition pore (mPTP) and necrosis (56, 57). However, our results suggest that DMSO-induced cell death is mPTP independent. Furthermore, as shown in Fig. 5, DMSO-induced cell death increased expression of Bax in mitochondrial extracts at final concentrations of 2 and 4 but not 1% (v/v), up to 24 h after exposure. This observation is in agreement with the existing literature where 1% DMSO treatment for up to 40 h in U937 cells (the human myeloid leukemia cell line) did not show changes in Bax levels (46). Likewise, in an *in vivo* model, Dalton's lymphoma mice mRNA levels were assessed and the levels of Bax increased with the concomitant decrease of the Bcl-2/Bax ratio after DMSO treatment (7.5 g/kg ip; ref. 58).

Our results show that DMSO-induced cell death is caspase-3 independent. This differs from results obtained previously in hepatocytes (59) and *in vivo* in the central nervous system (6). In this study, results obtained in the brain of mice treated with DMSO show caspase-3 activation in brain slices of different regions of the brain (6). At first glance, the data presented in this study appear to contradict these findings. However, Hanslick *et al.* (6) postulate that a possible source of the detected caspase-3 activation could be astrocytes or other glia-like cells, as white matter was predominantly stained. Since caspase-3 activation was not colocalized with a neuronal marker in their study, further work is needed to confirm this hypothesis.

DMSO-induced RGC-5 cell death appeared AIF dependent as DMSO induced a significant degree of AIF translocation from mitochondria to the nucleus 24 h after exposure to 2 or 4% (v/v) DMSO. A number of cytotoxic drugs used to induce cell death, *N*-methyl-D-aspartic acid (NMDA), glutamate, methylnitronitrosoguanidine (MNNG), hydrogen peroxide (H_2O_2), serum withdraw, staurosporine, glucocorticoids, adriamycin, cisplatin, ceramide, and etoposide (topoisomerase II inhibitor), have been shown to cause cleavage of AIF and its release from mitochondria and translocation to the nucleus (60–63). This is, however, to our knowledge, the first occasion that AIF release and translocation from the mitochondria to the nucleus following treatment with DMSO has been reported. AIF

has been previously linked to the activation of PARP-1 in the pathway to cell death (62–64). Figures 5 and 6 indicate that a simultaneous increase in PARP-1 activation 24 h after exposure to 2, 4, and 8% (v/v) DMSO and nuclear AIF after 2 and 4% (v/v) DMSO. Increased PARP expression has also been described *in vivo*, following DMSO treatment in Dalton's lymphoma mice (58).

AIF and PARP-1 activation have been previously implicated in caspase-independent cell death, through a newly proposed pathway of cell death: Parthanatos (65, 66). Parthanatos is a form of apoptosis associated with rapid activation of PARP-1 with early accumulation of poly-(ADP-ribose) (PAR) polymers, mitochondria depolarization, loss of NAD and ATP, late caspase-3 activation (although not necessary for cell death), PI cell permeabilization within 18–24 h of onset, and calpain-independent AIF activation (52, 61, 67–69). In this study, we see PARP-1 activation, AIF translocation, and mitochondrial respiration inhibition in accordance with what is described for Parthanatos cell death. Despite being a strong candidate, particularly as we do not see caspase-3 activation during the 24 h treatment, we do not believe that we are observing the Parthanatos pathway of cell death in response to low concentrations of DMSO. PI staining is a good indicator of plasma membrane permeabilization, and our results showed that there was little evidence of this <8% (24 h) despite the observed cell death (Fig. 4). In addition, it has been noted that inhibition of PARP-1-dependent cell death by CsA after MNNG treatment affects Parthanatos (37); our data indicate that CsA does not decrease cell death after DMSO treatment (data not shown). Since there is no evidence for mPTP involvement in response to low concentrations (<8% v/v) of DMSO, no changes to NADH levels and no PI staining within 24 h of the DMSO insult, this suggests that low concentrations of DMSO induced a cell death pathway that differs from the Parthanatos pathway (Fig. 7).

AIF and Bax have been implicated in the Fas-induced cell death pathway (70). Furthermore, Fas levels were reported to be elevated after DMSO treatment in the human myeloid leukemia cell line (47). In the eye, Fas-mediated cell death has been reported though activation of Fas/FasL to glia (71, 72) and *in vitro* RGC-5 apoptosis has been shown to occur in coculture with activated T cells (73). Neither glial or T cells were present in our *in vitro* study, which is therefore unlikely to involve Fas.

We propose that the mechanism by which DMSO induces cell death (Fig. 7) involves inhibition of mitochondrial respiration leading to decreased oxygen consumption within minutes of application. Moreover, elevation of cytosolic calcium and phosphatidylserine externalization occur. Calcium has been implicated in phosphatidylserine flipping previously (74–76) and is known to induce calpain activation (77, 78). Calpain acts to induce the release and redistribution of AIF to the nucleus (77, 78). This could occur through Bax-translocation from the cytosol to the mitochondria (79, 80). Increased levels of Bax in mitochondrial fractions and decreased levels in the cytosolic fractions are in accordance with Bax oligomerization and pore formation indicating that AIF translocation from mitochondria is *via* Bax pore formation (Fig. 5). AIF has also been implicated in phosphatidylserine externalization through the interaction with scramblase Scrm-1 (81). AIF can in addiction translocate to the nucleus and cause DNA fragmentation and activation of PARP-1 (Figs. 5 and 6) leading to cell death (Fig. 2).

DMSO is a universal solvent routinely used in experimental and biological disciplines, and is widely accepted to be nontoxic at concentrations <10% (v/v; refs. 8, 9, 12, 14–19, 42). It is often used to solubilize drug molecules that are otherwise poorly soluble. Our finding that at concentrations <10% (v/v), DMSO is toxic is unexpected. These results underline safety concerns of using low concentrations of DMSO as a solvent for *in vivo* administration of numerous molecules, which we show not to be safe. We believe that the scientific community should question the use of DMSO in biological assays, with particular relevance to delivery to neuronal cells. Finally, due to the broad number of drugs dissolved in DMSO, we believe these results have widespread implications, not only in the eye and in neuroscience, but also throughout the whole body.

Given the ubiquitous use of DMSO in biological assays, we would like to highlight to the scientific community the implications of our results. We recommend that other methods (such as micelle/liposomal formulations) are used in preference to DMSO for solubilizing drugs, but where no alternative exists, absolute DMSO concentrations are calculated and reported. We recommend that the percentage of DMSO used to dissolve drugs should be kept to a minimum (injection of <1% v/v solutions *in vivo*), and an untreated control group is included in addition to DMSO vehicle control to check for solvent toxicity. FJ

This study was supported by Foundation for Science and Technology, Portugal (FCT Fellowship SFRH/BD/47947/2008) and Fonds Européen de Développement Régional (FEDER). The authors thank Dr. Lisa Turner for proofreading; Dr. Will Kotiadis, Dr. Ronan Astin, and Dr. Goncalo Pereira for help using the mitochondrial respiration electrode; and Dr. António Francisco Ambrósio and Dr. Ana Raquel Santiago for general advice. Conflict of interest: M.F.C. has a patent application.

REFERENCES

1. Szmant, H. H. (1975) Physical properties of dimethyl sulfoxide and its function in biological systems. *Ann. N. Y. Acad. Sci.* **243,** 20–23
2. Sankpal, U. T., Abdelrahim, M., Connelly, S. F., Lee, C. M., Madero-Visbal, R., Colon, J., Smith, J., Safe, S., Maliakal, P., and Basha, R. (2012) Small molecule tolfenamic acid inhibits PC-3 cell proliferation and invasion in vitro and tumor growth in orthotopic mouse model for prostate cancer. *Prostate* **72,** 1648–1658
3. Modesitt, S. C., and Parsons, S. J. (2010) In vitro and in vivo histone deacetylase inhibitor therapy with vorinostat and pacli-

taxel in ovarian cancer models: does timing matter? *Gynecol. Oncol.* **119,** 351–357
4. Li, Y., and Lo, A. C. (2012) Lutein protects RGC-5 cells against hypoxia and oxidative stress. *Int. J. Mol. Sci.* **11,** 2109–2117
5. Julien, C., Marcouiller, F., Bretteville, A., El Khoury, N. B., Baillargeon, J., Hébert, S. S., and Planel, E. (2012) Dimethyl sulfoxide induces both direct and indirect tau hyperphosphorylation. *PLoS One* **7,** e40020
6. Hanslick, J. L., Lau, K., Noguchi, K. K., Olney, J. W., Zorumski, C. F., Mennerick, S., and Farber, N. B. (2009) Dimethyl sulfoxide (DMSO) produces widespread apoptosis in the developing central nervous system. *Neurobiol. Dis.* **34,** 1–10
7. Sun, H. H., Saheb-Al-Zamani, M., Yan, Y., Hunter, D. A., Mackinnon, S. E., and Johnson, P. J. (2012) Geldanamycin accelerated peripheral nerve regeneration in comparison to FK-506 in vivo. *Neuroscience* **223,** 114–123
8. Pelzel, H. R., Schlamp, C. L., and Nickells, R. W. (2010) Histone H4 deacetylation plays a critical role in early gene silencing during neuronal apoptosis. *BMC Neurosci.* **11,** 62
9. Pelzel, H. R., Schlamp, C. L., Waclawski, M., Shaw, M. K., and Nickells, R. W. (2012) Silencing of Fem1cR3 gene expression in the DBA/2J mouse precedes retinal ganglion cell death and is associated with histone deacetylase activity. *Invest. Ophthalmol. Vis. Sci.* **53,** 1428–1435
10. Lin, Yang J, Lin J, Lai K, and Lu, H. (2011) Rutin inhibits human leukemia tumor growth in a murine xenograft model. *In Vivo* **2011,** 1–5
11. Teng, B. T., Tam, E. W., Benzie, I. F., and Siu, P. M. (2011) Protective effect of caspase inhibition on compression-induced muscle damage. *J. Physiol.* **589,** 3349–3369
12. Avila, M. Y., Seidler, R. W., Stone, R. A., and Civan, M. M. (2002) Inhibitors of NHE-1 Na^+/H^+ exchange reduce mouse intraocular pressure. *Invest. Ophthalmol. Vis. Sci.* **43,** 1897–1902
13. Hill, R. V. (1973) Dimethyl sulfoxide in the treatment of retinal disease. *Ann. N. Y. Acad. Sci.* **243,** 485–90
14. Piña, Y., Decatur, C., Murray, T., Houston, S., Gologorsky, D., Cavalcante, M., Hernandez, E., Celdran, M., Feuer, W., and Lampidis, T. (2011) Advanced retinoblastoma treatment: targeting hypoxia by inhibition of the mammalian target of rapamycin (mTOR) in LH(BETA)T(AG) retinal tumors. *Clin. Ophthalmol.* **5,** 337–343
15. Lüke, J., Nassar, K., Lüke, M., Tura, A., Merz, H., Giannis, A., and Grisanti, S. (2010) The effect of adjuvant dimethylenastron, a mitotic Kinesin Eg5 inhibitor, in experimental glaucoma filtration surgery. *Curr. Eye Res.* **35,** 1090–1098
16. Burugula, B., Ganesh, B. S., and Chintala, S. K. (2011) Curcumin attenuates staurosporine-mediated death of retinal ganglion cells. *Invest. Ophthalmol. Vis. Sci.* **52,** 4263–4273
17. Rojas, J. C., Lee, J., John, J. M., and Gonzalez-Lima, F. (2008) Neuroprotective effects of near-infrared light in an in vivo model of mitochondrial optic neuropathy. *J. Neurosci.* **28,** 13511–13521
18. Rojas, J. C., Saavedra, J. A., and Gonzalez-Lima, F. (2008) Neuroprotective effects of memantine in a mouse model of retinal degeneration induced by rotenone. *Brain Res.* **1215,** 208–217
19. Konno, T., Uchibori, T., Nagai, A., Kogi, K., and Nakahata, N. (2007) Effect of 2-(6-cyano-1-hexyn-1-yl)adenosine on ocular blood flow in rabbits. *Life Sci.* **80,** 1115–1122
20. Fischer, U. T., and Schulze-Osthoff, K. (2005) New approaches and therapeutics targeting apoptosis in disease. *Pharmacol. Rev.* **57,** 187–215
21. Hengartner, M. O. (2000) The biochemistry of apoptosis. *Nature* **407,** 770–776
22. Reed, J. C. (2000) Mechanisms of apoptosis. *Am. J. Pathol.* **157,** 1415–1430
23. Notman, R., Noro, M., O'Malley, B., and Anwar, J. (2006) Molecular basis for dimethylsulfoxide (DMSO) action on lipid membranes. *J. Am. Chem. Soc.* **128,** 13982–13983
24. De Ménorval, M.-A., Mir, L. M., Fernández, M. L., and Reigada, R. (2010) Effects of dimethyl sulfoxide in cholesterol-containing lipid membranes: a comparative study of experiments in silico and with cells. *PLoS One* **7,** e41733
25. Liu, J., Yoshikawa, H., Nakajima, Y., and Tasaka, K. (2001) Involvement of mitochondrial permeability transition and caspase-9 activation in dimethyl sulfoxide-induced apoptosis of EL-4 lymphoma cells. *Int. Immunopharmacol.* **1,** 63–74
26. Qi, W., Ding, D., and Salvi, R. J. (2008) Cytotoxic effects of dimethyl sulphoxide (DMSO) on cochlear organotypic cultures. *Hear. Res.* **236,** 52–60
27. Cordeiro, M. F., Guo, L., Luong, V., Harding, G., Wang, W., Jones, H. E., Moss, S. E., Sillito, A. M., and Fitzke, F. W. (2004) Real-time imaging of single nerve cell apoptosis in retinal neurodegeneration. *Proc. Natl. Acad. Sci. U. S. A.* **101,** 13352–13366
28. Bizrah, M., Dakin, S. C., Guo, L., Rahman, F., Parnell, M., Normando, E., Nizari, S., and Younis, A. (2012) Validation and refinement of an automated technique of counting apoptosing retinal cells imaged with DARC. *Invest. Ophthalmol. Vis. Sci.* **53,** ARVO Abstract 1175
29. Krishnamoorthy, R. R., Agarwal, P., Prasanna, G., Vopat, K., Lambert, W., Sheedlo, H. J., Pang, I. H., Shade, D., Wordinger, R. J., Yorio, T., Clark, A. F., and Agarwal, N. (2001) Characterization of a transformed rat retinal ganglion cell line. *Brain Res. Mol. Brain Res.* **86,** 1–12
30. Nadal-Nicolás, F. M., Jiménez-López, M., Sobrado-Calvo, P., Nieto-López, L., Cánovas-Martínez, I., Salinas-Navarro, M., Vidal-Sanz, M., and Agudo, M. (2009) Brn3a as a marker of retinal ganglion cells: qualitative and quantitative time course studies in naive and optic nerve-injured retinas. *Invest. Ophthalmol. Vis. Sci.* **50,** 3860–3888
31. Van Bergen, N. J., Wood, J. P., Chidlow, G., Trounce, I. A., Casson, R. J., Ju, W.-K., Weinreb, R. N., and Crowston, J. G. (2009) Recharacterization of the RGC-5 retinal ganglion cell line. *Invest. Ophthalmol. Vis. Sci.* **50,** 4267–4272
32. Liu, B., Sun, X., Suyeoka, G., Garcia, J. G., and Leiderman, Y. I. (2013) TGFβ signaling induces expression of Gadd45b in retinal ganglion cells. *Invest. Ophthalmol. Vis. Sci.* **54,** 1061–1069
33. Balaiya, S., Ferguson, L. R., and Chalam, K. V. (2013) Evaluation of sirtuin role in neuroprotection of retinal ganglion cells in hypoxia. *Invest. Ophthalmol. Vis. Sci.* **53,** 4315–4322
34. Santiago, A. R., Cristóvão, A. J., Santos, P. F., Carvalho, C. M., and Ambrósio, A. F. (2007) High glucose induces caspase-independent cell death in retinal neural cells. *Neurobiol. Dis.* **25,** 464–472
35. Kumi-Diaka, J., and Butler, A. (2000) Caspase-3 protease activation during the process of genistein-induced apoptosis in TM4 testicular cells. *Biol. Cell* **92,** 115–124
36. Elmore S. (2007) Apoptosis: a review of programmed cell death. *Toxicol. Pathol.* **35,** 495–516
37. Van Wijk, S. J., and Hageman, G. J. (2005) Poly(ADP-ribose) polymerase-1 mediated caspase-independent cell death after ischemia/reperfusion. *Free Radic. Biol. Med.* **39,** 81–90
38. Abeti, R., and Duchen, M. R. (2012) Activation of PARP by oxidative stress induced by β-amyloid: implications for Alzheimer's disease. *Neurochem. Res.* **37,** 2589–2596
39. Avila, M. Y., Stone, R. A., and Civan, M. M. (2002) Knockout of A3 adenosine receptors reduces mouse intraocular pressure. *Invest. Ophthalmol. Vis. Sci.* **43,** 3021–3026
40. Aita, K., Irie, H., Tanuma, Y., Toida, S., Okuma, Y., Mori, S., and Shiga, J. (2005) Apoptosis in murine lymphoid organs following intraperitoneal administration of dimethyl sulfoxide (DMSO). *Exp. Mol. Pathol.* **79,** 265–271
41. Ekwall, B., Silano, V., and Zucco, F. (1990) Toxicity tests with mammalian cell cultures. In *Short-Term Toxicity Tests for Non-genotoxic Effects* (Bourdeau, P., Somers, E., Richardson, G. M., andHickman, J. R., eds) pp. 75–98, John Wiley & Sons, Chichester/New York/Brisbane/Toronto/Singapore
42. Huang, Y., Li, Z., Wang, N., van Rooijen, N., and Cui, Q. (2008) Roles of PI3K and JAK pathways in viability of retinal ganglion cells after acute elevation of intraocular pressure in rats with different autoimmune backgrounds. *BMC Neurosci.* **9,** 78
43. Li, B., Yang, C., Rosenbaum, D. M., and Roth, S. (2000) Signal transduction mechanisms involved in ischemic preconditioning in the rat retina in vivo. *Exp. Eye Res.* **70,** 755–765
44. Perche, O., Doly, M., and Ranchon,-Cole, I. (2007) Caspase-dependent apoptosis in light-induced retinal degeneration. *Invest. Ophthalmol. Vis. Sci.* **48,** 2753–2759
45. Daniels, S. A., Coonley, K. G., and Yoshizumi, M. O. (1990) Taxol treatment of experimental proliferative vitreoretinopathy. *Graefes Arch. Clin. Exp. Ophthalmol.* **228,** 513–516
46. Tsai, T. I., Bui, B. V., and Vingrys, A. J. (2009) Dimethyl sulphoxide dose-response on rat retinal function. *Doc. Ophthalmol.* **119,** 199–207

47. Vondrácek, J., Soucek, K., Sheard, M. A., Chramostová, K., Andrysík, Z., Hofmanová, J., and Kozubík, A. (2006) Dimethyl sulfoxide potentiates death receptor-mediated apoptosis in the human myeloid leukemia U937 cell line through enhancement of mitochondrial membrane depolarization. *Leuk. Res.* **30,** 81–89
48. Cao, X.-G., Li, X.-X., Bao, Y.-Z., Xing, N.-Z., and Chen, Y. (2007) Responses of human lens epithelial cells to quercetin and DMSO. *Invest. Ophthalmol. Vis. Sci.* **48,** 3714–3718
49. Zacharias, L. C., Estrago-Franco, M. F., Ramirez, C., and Kenney, M. C. (2011) The effects of commercially available preservative-free FDA-approved triamcinolone (Triesence) on retinal cells in culture. *J. Ocul. Pharmacol. Ther.* **27,** 143–150
50. Yu, Z. W., and Quinn, P. J. (1994) Dimethyl sulphoxide: a review of its applications in cell biology. *Biosci. Rep.* **14,** 259–281
51. Clerc, P., and Polster, B. M. (2012) Investigation of mitochondrial dysfunction by sequential microplate-based respiration measurements from intact and permeabilized neurons. *PLoS One* **7,** e34465.
52. Andrabi, S. A., Dawson, T. M., and Dawson, V. L. (2008) Mitochondrial and nuclear cross talk in cell death: parthanatos. *Ann. N. Y. Acad. Sci.* **1147,** 233–241
53. Sun, C., Guo, X.-X., Zhu, D., Xiao, C., Bai, X., Li, Y., Zhan, Z., Li, X.-L., Song, Z.-G., and Jin, Y.-H. (2013) Apoptosis is induced in cancer cells via the mitochondrial pathway by the novel xylocydine-derived compound JRS-15. *Int. J. Mol. Sci.* **14,** 850–870
54. Brown, H. M., and Rydqvist, B. (1990) Dimethyl sulfoxide elevates intracellular Ca^{2+} and mimics effects of increased light intensity in a photoreceptor. *Plügers Arch.* **415,** 395–398
55. Osellame, L. D., Blacker, T. S., and Duchen, M. R. (2012) Cellular and molecular mechanisms of mitochondrial function. *Best Pract. Res. Clin. Endocrinol. Metab.* **26,** 711–723
56. Duchen, M. R. (2012) Mitochondria, calcium-dependent neuronal death and neurodegenerative disease. *Pflügers Arch.* **464,** 111–121
57. Halestrap, A. P. (1999) The mitochondrial permeability transition: its molecular mechanism and role in reperfusion injury. *Biochem. Soc. Symp.* **66,** 181–203
58. Koiri, R. K., and Trigun, S. K. (2011) Dimethyl sulfoxide activates tumor necrosis factorα-p53 mediated apoptosis and down regulates D-fructose-6-phosphate-2-kinase and lactate dehydrogenase-5 in Dalton's lymphoma in vivo. *Leuk. Res.* 35, 950–956
59. Banič, B., Nipič, D., Suput, D., and Milisav, I. (2011) DMSO modulates the pathway of apoptosis triggering. *Cell. Mol. Biol. Lett.* **16,** 328–341
60. Delavallée, L., Cabon, L., Galán-Malo, P., Lorenzo, H. K., and Susin, S. A. (2011) AIF-mediated caspase-independent necroptosis: a new chance for targeted therapeutics. *IUBMB Life* **63,** 221–232
61. Yu, S. W., Wang, H., Poitras, M. F., Coombs, C., Bowers, W. J., Federoff, H. J., Poirier, G. G., Dawson, T. M., and Dawson, V. L. (2002) Mediation of poly(ADP-ribose) polymerase-1-dependent cell death by apoptosis-inducing factor. *Science* **297,** 259–263
62. Daugas, E., Susin, S. A., Zamzami, N., Ferri, K. F., Irinopoulou, T., Larochette, N., Prévost, M. C., Leber, B., Andrews, D., Penninger, J., and Kroemer, G. (2000) Mitochondrio-nuclear translocation of AIF in apoptosis and necrosis. *FASEB J.* **14,** 729–739
63. Lorenzo, H. K., Susin, S. A, Penninger, J., and Kroemer, G. (1999) Apoptosis inducing factor (AIF): a phylogenetically old, caspase-independent effector of cell death. *Cell Death Differ.* **6,** 516–524
64. Hong, S. J., Dawson, T. M., and Dawson, V. L. (2004) Nuclear and mitochondrial conversations in cell death: PARP-1 and AIF signaling. *Trends Pharmacol. Sci.* **25,** 259–264
65. Wang, Y., Kim, N. S., Haince, J.-F., Kang, H. C., David, K. K., Andrabi, S. A., Poirier, G. G., Dawson, V. L., and Dawson, T. M. (2011) Poly(ADP-ribose) (PAR) binding to apoptosis-inducing factor is critical for PAR polymerase-1-dependent cell death (parthanatos). *Sci. Signal.* **4,** ra20
66. Wang, Y., Dawson, V. L., and Dawson, T. M. (2009) Poly(ADP-ribose) signals to mitochondrial AIF: a key event in parthanatos. *Exp. Neurol.* **218,** 193–202
67. Andrabi, S. A., Kim, N. S., Yu, S.-W., Wang, H., Koh, D. W., Sasaki, M., Klaus, J. A., Otsuka, T., Zhang, Z., Koehler, R. C., Hurn, P. D., Poirier, G. G., Dawson, V. L., and Dawson, T. M. (2006) Poly(ADP-ribose) (PAR) polymer is a death signal. *Proc. Natl. Acad. Sci. U. S. A.* **103,** 18308–18313
68. Yu, S. W., Andrabi, S. A., Wang, H., Kim, N. S., Poirier, G. G., Dawson, T. M., and Dawson, V. L. (2006) Apoptosis-inducing factor mediates poly(ADP-ribose) (PAR) polymer-induced cell death. *Proc. Natl. Acad. Sci. U. S. A.* **103,** 18314–18319
69. Wang, Y., Kim, N. S., Li, X., Greer, P. A., Koehler, R. C., Dawson, V. L., and Dawson, T. M. (2009) Calpain activation is not required for AIF translocation in PARP-1-dependent cell death (parthanatos). *J. Neurochem.* **110,** 687–696
70. Austin, J. W., and Fehlings, M. G. Molecular mechanisms of Fas-mediated cell death in oligodendrocytes. (2008) *J. Neurotrauma* **25,** 411–426
71. Gregory, M. S., Hackett, C. G., Abernathy, E. F., Lee, K. S., Saff, R. R., Hohlbaum, A. M., Moody, K. S., Hobson, M. W., Jones, A., Kolovou, P., Karray, S., Giani, A., John, S. W., Chen, D. F., Marshak-Rothstein, A., and Ksander, B. R. (2011) Opposing roles for membrane bound and soluble Fas ligand in glaucoma-associated retinal ganglion cell death. *PLoS One* **6,** e17659
72. Ju, K. R., Kim, H. S., Kim, J. H., Lee, N. Y., and Park, C. K. (2006) Retinal glial cell responses and Fas/FasL activation in rats with chronic ocular hypertension. *Brain Res.* **1122,** 209–221
73. Wax, M. B., Tezel, G., Yang, J., Peng, G., Patil, R. V., Agarwal, N., Sappington, R. M., and Calkins, D. J. (2009) Induced autoimmunity to heat shock proteins elicits glaucomatous loss of retinal ganglion cell neurons via activated T cell-derived Fas-ligand. *J. Neurosci.* **28,** 12085–12096
74. Lee, S. H., Meng, X. W., Flatten, K. S., Loegering, D. A., and Kaufmann, S. H. (2013) Phosphatidylserine exposure during apoptosis reflects bidirectional trafficking between plasma membrane and cytoplasm. *Cell Death Differ.* **20,** 64–76
75. Mirnikjoo, B., Balasubramanian, K., and Schroit, A. J. (2009) Mobilization of lysosomal calcium regulates the externalization of phosphatidylserine during apoptosis. *J. Biol. Chem.* **284,** 6918–6923
76. Mirnikjoo, B., Balasubramanian, K., and Schroit, A. J. (2009) Suicidal membrane repair regulates phosphatidylserine externalization during apoptosis. *J. Biol. Chem.* **284,** 22512–22516
77. Polster, B. M., Basañez, G., Etxebarria, A., Hardwick, J. M., and Nicholls, D. G. (2005) Calpain I induces cleavage and release of apoptosis-inducing factor from isolated mitochondria. *J. Biol. Chem.* **280,** 6447–6454
78. Norberg, E., Orrenius, S., and Zhivotovsky, B. (2010) Mitochondrial regulation of cell death: processing of apoptosis-inducing factor (AIF). *Biochem. Biophys. Res. Commun.* **396,** 95–100.
79. Vieira, H., and Kroemer, G. (2003) Mitochondria as targets of apoptosis regulation by nitric oxide. *IUBMB Life* **55,** 613–616
80. Er, E., Oliver, L., Cartron, P.-F., Juin, P., Manon, S., and Vallette, F. M. (2006) Mitochondria as the target of the pro-apoptotic protein Bax. *Biochim. Biophys. Acta* **1757,** 1301–1311
81. Wang, X., Wang, J., Gengyo-Ando, K., Gu, L., Sun, C.-L., Yang, C., Shi, Y., Kobayashi, T., Shi, Y., Mitani, S., Xie, X. S., and Xue, D. (2007) C. elegans mitochondrial factor WAH-1 promotes phosphatidylserine externalization in apoptotic cells through phospholipid scramblase SCRM-1. *Nat. Cell Biol.* **9,** 541–549

Received for publication June 17, 2013.
Accepted for publication November 26, 2013.